Electronic Supplementary Material (ESI) for Dalton Transactions.

Supporting Information

Intercalative Hybridization of Layered Double Hydroxide Nanocrystal with Mesoporous g-C_3N_4 for Enhancing Visible Light-Induced H_2 Production Efficiency

Jang Mee Lee,[a] Jae-Hoon Yang,[a] Nam Hee Kwon,[a] Yun Kyung Jo,[a] Jin-Ho Choy,[a] and Seong-Ju Hwang*,[a]

[a] Center for Hybrid Interfacial Chemical Structure (CICS), Department of Chemistry and Nanoscience, College of Natural Sciences, Ewha Womans University, Seoul 03760, Korea

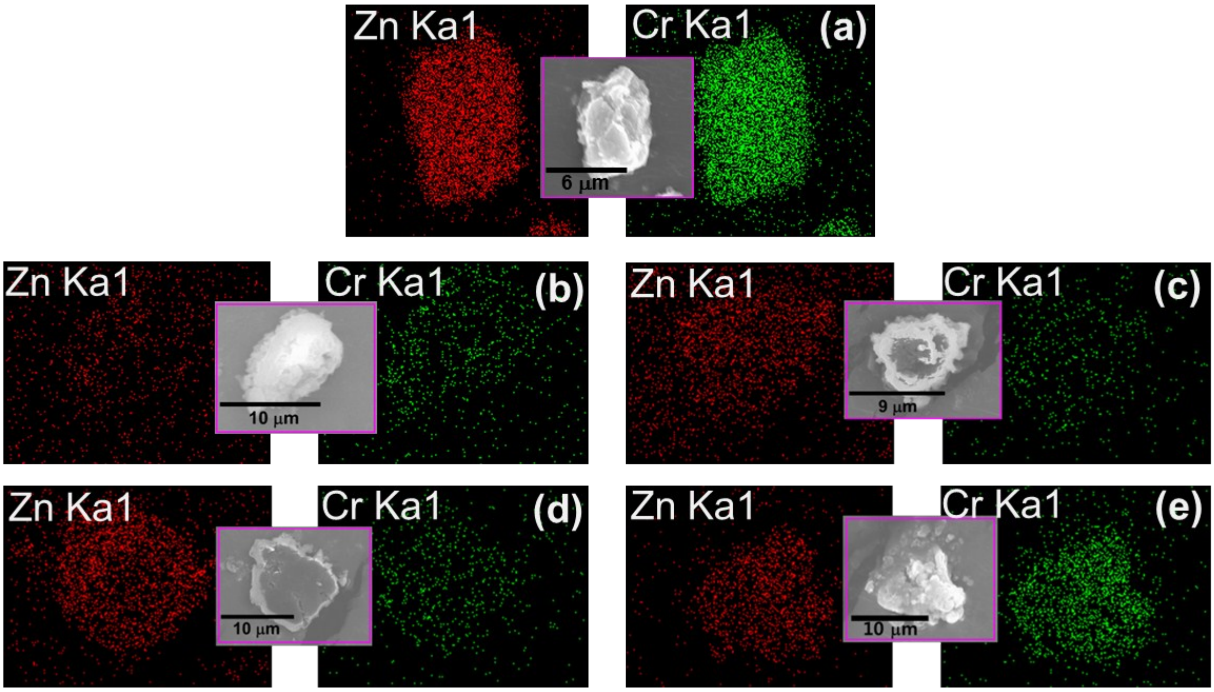

Figure S1. Energy dispersive spectrometry (EDS)–elemental maps and (center) FE-SEM images of (a) the pristine Zn–Cr-layered double hydroxide (LDH), (b) **ZCCN1**, (c) **ZCCN2**, (d) **ZCCN3**, and (e) **ZCCN4**.

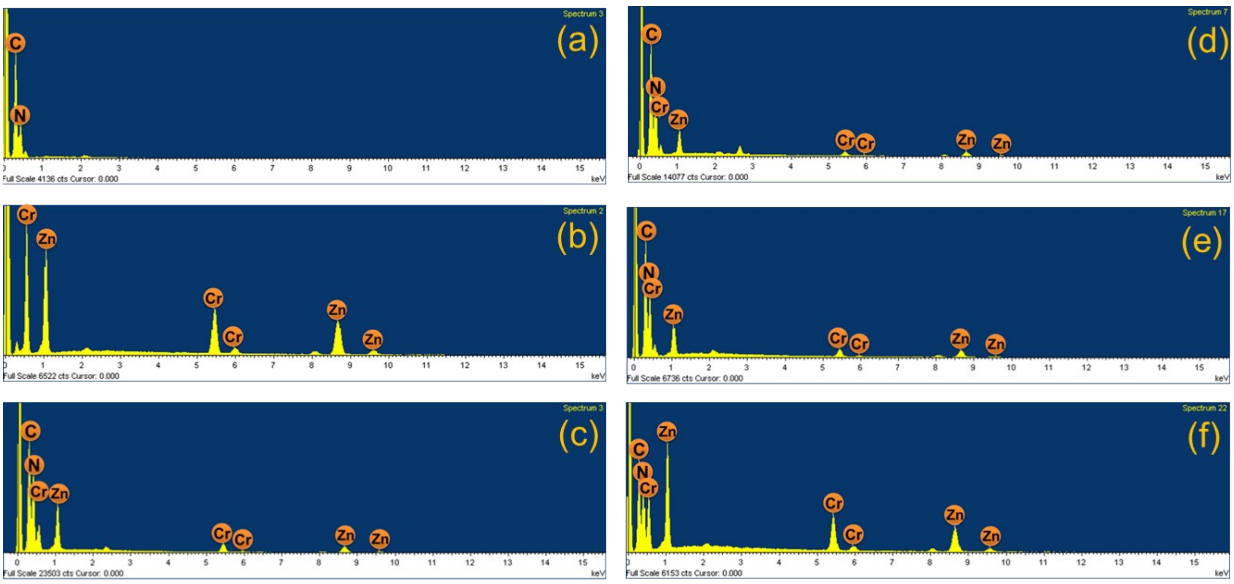

Figure S2. EDS results of the Zn–Cr-LDH–g-C_3N_4 nanohybrids of (a) the pristine g-C_3N_4, (b) Zn–Cr-LDH, (c) **ZCCN1**, (d) **ZCCN2**, (e) **ZCCN3**, and (f) **ZCCN4**.

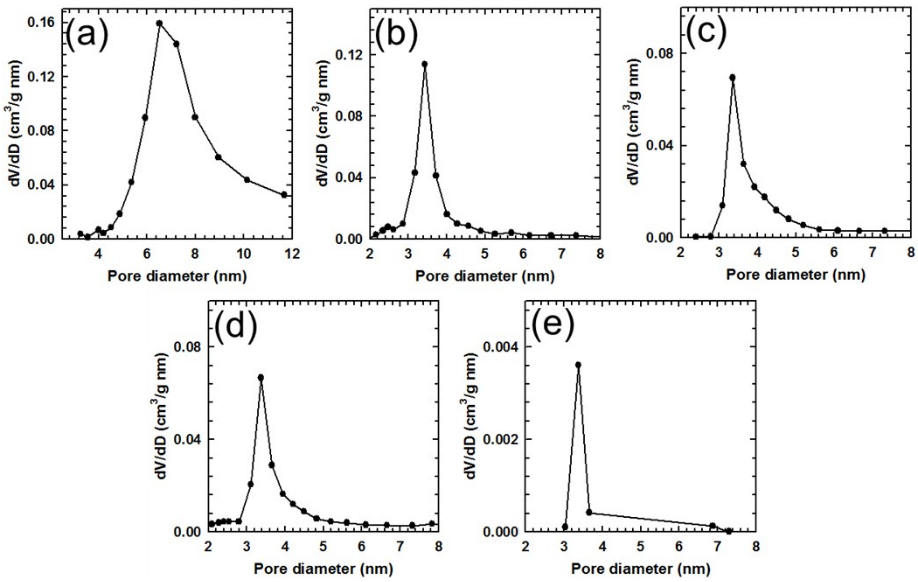

Figure S3. Pore size distribution curves of (a) mesoporous g-C_3N_4 and the Zn–Cr-LDH–g-C_3N_4 nanohybrids of (b) **ZCCN1**, (c) **ZCCN2**, (d) **ZCCN3**, and (e) **ZCCN4**.

g-C_3N_4		**ZCCN1**		**ZCCN2**		**ZCCN3**		**ZCCN4**	
BE (eV)	**Area (%)**	**BE (eV)**	**Area (%)**	**BE (eV)**	**Area (%)**	**BE (eV)**	**Area (%)**	**BE (eV)**	**Area (%)**
284.60	7.4	284.60	25.9	284.60	20.4	284.60	22.9	284.60	33.7
286.18	8.6	286.27	8.3	286.24	9.0	286.20	10.1	286.16	7.7
287.92	84.0	288.04	65.8	287.90	70.5	287.84	66.9	287.98	58.6

g-C_3N_4		**ZCCN1**		**ZCCN2**		**ZCCN3**		**ZCCN4**	
BE (eV)	**Area (%)**	**BE (eV)**	**Area (%)**	**BE (eV)**	**Area (%)**	**BE (eV)**	**Area (%)**	**BE (eV)**	**Area (%)**
398.42	76.9	398.55	79.5	398.41	78.8	398.35	79.4	398.48	77.5
399.73	4.2	399.88	5.9	399.71	6.4	399.65	3.2	399.73	5.7
400.44	18.9	400.70	14.6	400.54	14.8	400.36	17.4	400.55	16.8

Table S1. Results of deconvolution analysis for (top) C and (bottom) N 1s X-ray photoelectron spectra (XPS) of the pristine g-C_3N_4 and the Zn–Cr-LDH–g-C_3N_4 nanohybrids

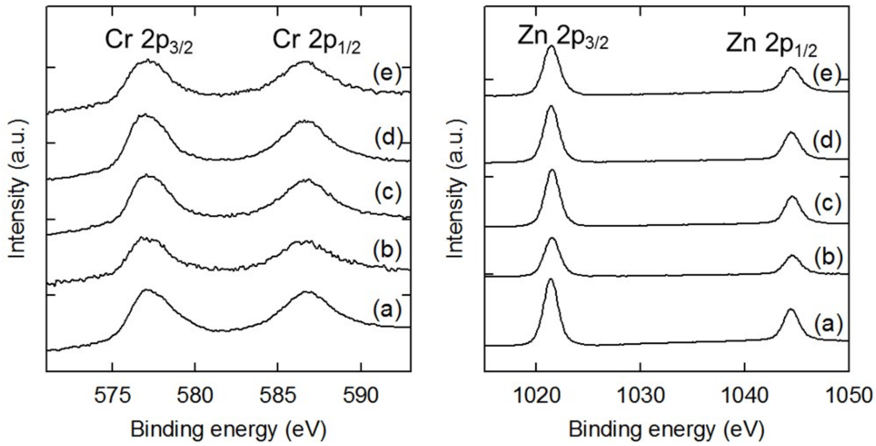

Figure S4. (Left) Cr 2p and (right) Zn 2p XPS data of (a) the pristine Zn–Cr-LDH and the Zn–Cr-LDH–g-C_3N_4 nanohybrids of (b) **ZCCN1**, (c) **ZCCN2**, (d) **ZCCN3**, and (e) **ZCCN4**.

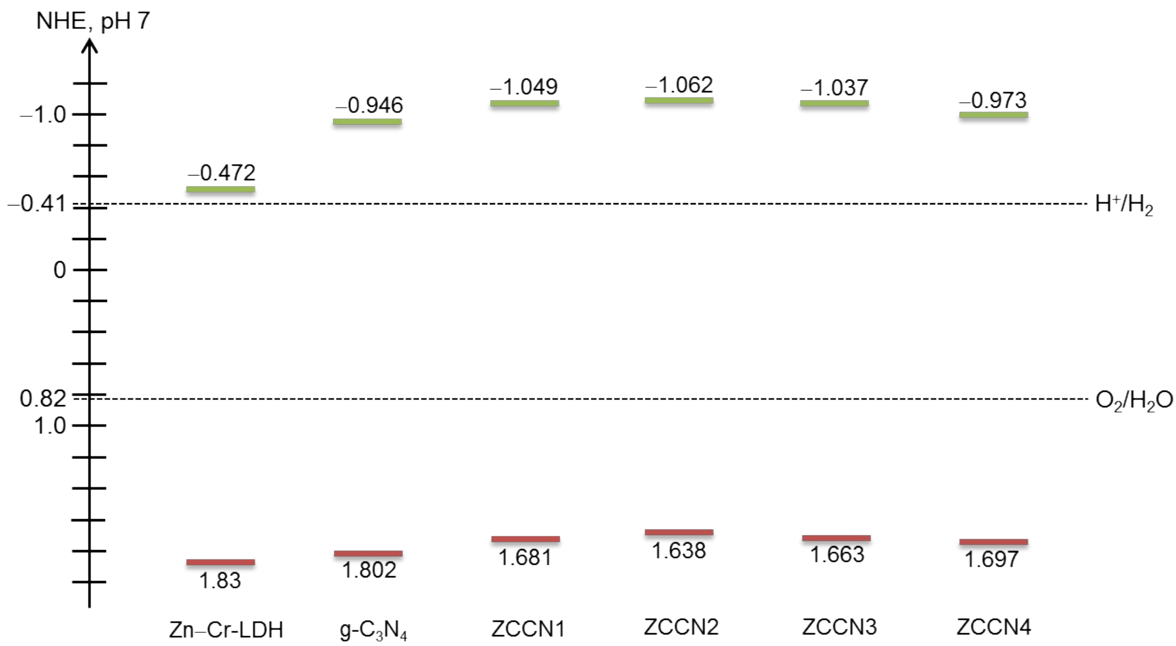

Figure S5. Energy band diagrams of the pristine Zn–Cr-LDH, the pristine g-C_3N_4, and the nanohybrids of **ZCCN1**, **ZCCN2**, **ZCCN3**, and **ZCCN4**.

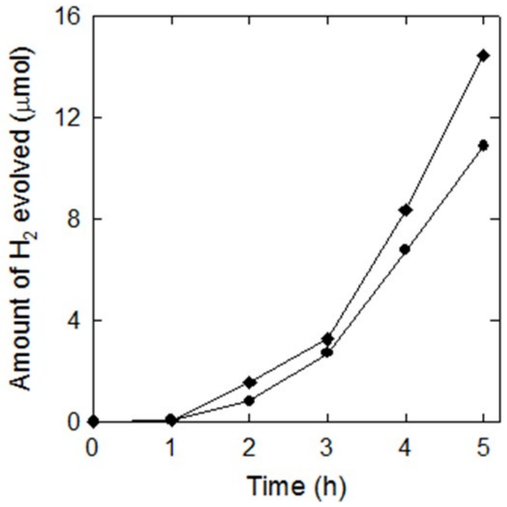

Figure S6. Time-dependent H_2 production under visible light irradiation ($\lambda > 420$ nm) of the physical mixture of g-C_3N_4 and Zn–Cr-LDH (squares), and g-C_3N_4 (circles).

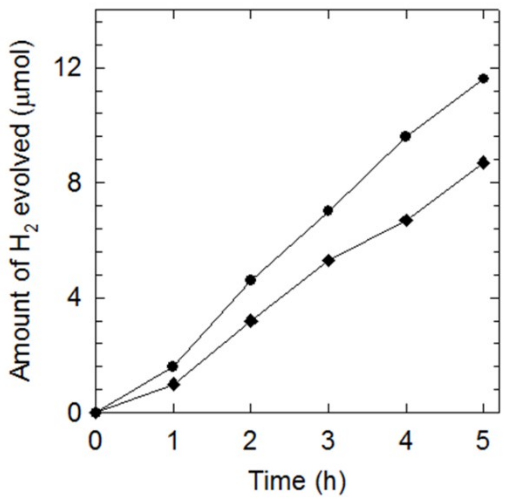

Figure S7. Time-dependent H_2 production under visible light irradiation ($\lambda > 420$ nm) of the nanohybrid of nonporous g-C_3N_4 and Zn–Cr-LDH (squares), and nonporous g-C_3N_4 (circles).